



## ANALYSIS OF COSMIC MATERIALS: RESULTS ON CARBON AND SILICATE LABORATORY ANALOGUES

L. Colangeli<sup>1</sup>, J.R. Brucato<sup>1</sup>, L. Ferrini<sup>1</sup>, V. Mennella<sup>1</sup>, E. Bussoletti<sup>2</sup>, P. Palumbo<sup>2</sup>, A. Rotundi<sup>2</sup>

<sup>1</sup>*Osservatorio Astronomico di Capodimonte, Via Moiarriello 16, 80131 Napoli, Italy*

<sup>2</sup>*Istituto Universitario Navale, Via A. de Gasperi 5, 80133 Napoli, Italy*

### ABSTRACT

Carbon and silicates are two of the main components of cosmic dust. They change nature through different evolutionary phases, according to the cosmic environment and the experienced processing. To understand the evolution of cosmic materials the study of “laboratory analogues” represents a powerful tool. In this context, systematic analyses are performed at the cosmic physics laboratory of Naples on solid particles, synthesised and processed under carefully controlled conditions. Different kinds of carbon and silicate samples are produced under various environmental conditions and exposed to processes (e.g. thermal annealing, UV irradiation and ion bombardment). The comparative analysis of the results allows us to link intrinsic properties (such as chemical composition and structure) to the optical behaviour of grains. This study offers the opportunity to interpret observations concerning the composition of small bodies in the Solar System, such as spectroscopic results obtained for comets by the Infrared Space Observatory (ISO). Several open questions remain, however, unsolved and await results from new laboratory experiments.

©1999 COSPAR. Published by Elsevier Science Ltd.

### INTRODUCTION

Infrared spectroscopy is a powerful tool to investigate physical and chemical properties of materials present in different space environments. In particular, bands falling in the 3.3 - 3.4  $\mu\text{m}$  range are typical of C-H stretching vibrations, common to several carbon based materials. Since the first detection in comet 1P/Halley (Combes *et al.*, 1988) their attribution has moved from a solid state to a molecular origin. Methanol (Disanti, 1995) and ethane (Mumma *et al.*, 1996) have been considered promising carriers, depending on the actual comet. Similar bands are observed in the interstellar medium and around sources rich in UV flux. The detailed band position and profile indicate different origins. Sub-micron amorphous carbon grains are suitable to reproduce wide absorption bands dominated by the 3.4  $\mu\text{m}$  aliphatic component, while polycyclic aromatic hydrocarbons (PAH's) are appropriate to interpret the sharper emission of aromatic features falling around 3.3  $\mu\text{m}$ . These evidences clearly suggest that similar features may have significantly different origin, depending on space environment and material processing.

Something similar is true for silicates. For several years the amorphous form has been considered as the “only” possible state of silicates in space. Only in comets, crystalline silicate features were observed (e.g. Hanner *et al.*, 1994). Recent observations in the medium and far infrared (especially thanks to the ISO space-born observatory) have demonstrated that crystalline silicates are a non negligible component in

comets and circumstellar environments (Waelkens *et al.*, 1996; Waters *et al.*, 1996; Crovisier *et al.*, 1997; Malfait *et al.*, 1998). Also for these materials, then, the puzzle of a self-consistent description of their morphology, structure and chemistry at different evolutionary stages has become a key question concerning cosmic dust evolution.

The problem of cosmic dust composition and evolution must be considered also in the framework of the elemental abundance budget. Updated evaluations (e.g. Snow & Witt, 1996) have placed several interstellar dust models in a critical position (Mathis, 1996; Dwek, 1997). They must be improved to become again compatible with observational evidences. In particular, the revised values for carbon and oxygen abundance in the interstellar medium are  $190 < 10^6 (C/H) < 290$  (Cardelli *et al.*, 1996) and  $10^6 O/H \approx 500$  (Meyer *et al.*, 1998) respectively. In the case of comets, in situ analyses have provided clear indications about the actual dust composition. According to available data (Jessberger & Kissel, 1991), the overall composition of comets (Greenberg, 1998) seems compatible with the presence of about 26 % in mass of silicates, 23 % of complex organic refractory materials dominated by carbon and about 9 % of attogram carbonaceous grains and PAH's; the rest should be mainly water. In the case of cometary dust, however, the puzzle of the actual arrangement of the different components is still open. The exploration of Halley's comet has evidenced that two chemical phases (organic particles and Mg-rich silicates) are inter-dispersed; in some cases pure silicate grains were observed. The two alternatives, core-mantle or fluffy grain structure, are both compatible with observations. The interstellar grain models (e.g. Li and Greenberg, 1997) would favour the first hypothesis, while the in situ detection of pure silicate grains and the laboratory analyses of interplanetary dust particles seem consistent with a random, fluffy aggregation of different materials.

In this framework, the study of cosmic dust analogues plays a fundamental role. In fact, laboratory experiments on grains synthesised under carefully controlled conditions and subjected to processes similar to those expected in space can offer several keys for a quantitative interpretation of astronomical observations.

Our group, as well as other research teams, undertake synthesis and processing experiments on carbon based and silicate particles. The common aim is to disclose the relations between spectroscopic, morphological and structural properties of materials. Using this approach, it is possible to build a clear evolutionary reference frame, in which also astronomical observations may find a systematic interpretation.

In the present work we summarise some of the main experimental results and show relevant correlation in the view of finding evolutionary processes which are generally valid and applicable to cosmic dust.

## COSMIC DUST ANALOGUES IN OUR LABORATORY

Various forms of disordered carbon grains are condensed by arc discharge between amorphous carbon electrodes in a 10 mbar atmosphere of pure Ar (ACAR sample), pure H<sub>2</sub> (ACH2 sample) or Ar-H<sub>2</sub> mixed gases. Other carbon grains are obtained by burning benzene in air (BE sample) at normal conditions (Colangeli *et al.*, 1995, Mennella *et al.*, 1997a).

Crystalline forsterite, fayalite and enstatite grains are obtained by grinding minerals. The amorphous counterparts can be synthesised by bombarding the same solid minerals by a high power ( $\sim 10^8$  Wcm<sup>-2</sup>) laser (Nd-YAG @ 1.064  $\mu$ m) in a 10 mbar O<sub>2</sub> atmosphere.

The produced samples are characterised in morphology (e.g. size distribution and grain shapes) by scanning electron microscopy (SEM) and transmission electron microscopy (TEM). These methods offer also the possibility to investigate the intimate structure of particles to the extent allowed by the instrument resolution (few nm). The energy dispersive X-ray (EDX) analysis is used to characterise the elemental composition, while transmission spectroscopy is used to determine the optical properties in the range of interest. Actually, spectroscopy in the widest spectral range (from the far UV to the mm range) is appropriate to derive information on the structure of materials too, as the solid state properties determine the observed spectral behaviour.

Thermal annealing (Mennella *et al.*, 1995a,b), UV irradiation (Mennella *et al.*, 1996) and ion bombardment (Mennella *et al.*, 1997b) are methods applied to reproduce the processing mechanisms acting in space. Analyses of the samples, before and after treatments, evidence how different mechanisms may affect the physical and chemical characteristics of our cosmic dust analogues. A synthesis of the processing conditions is given in Table 1. We note that, while the thermal annealing can only roughly simulate the processing of grains in space, UV irradiation and ion bombardment are probably the most effective processes active in space. The doses used in our experiments must be compared to the rates expected in the interstellar medium (see Mennella *et al.*, 1996, 1997b for more details). On a diffuse cloud time-scale (about  $3 \times 10^7$  yr.) the expected UV dose deposited in carbonaceous grains is about  $3 \times 10^{23}$  eV cm<sup>-2</sup> (Jenniskens, 1993), while the dose released by ion bombardment should not exceed about 30 eV/C-atom (Mennella *et al.*, 1997b).

Table 1. Processing of carbon based samples.

Technique	Processing conditions
Thermal annealing	Heating up to 800 °C @ $p < 10^{-5}$ mbar for 3 h (at each T step)
UV irradiation	doses: $5 \times 10^{20}$ , $1 \times 10^{22}$ and $4 \times 10^{22}$ eV cm <sup>-2</sup> hydrogen flow discharge lamp with MgF <sub>2</sub> window, $p = 2$ mbar
Ion bombardment	doses: 6.6, 66, 660 eV/C-atom beam of a 3 keV He <sup>+</sup> Varian ion gun low current of $1.5 \mu\text{A cm}^{-2}$ (very low sample heating)

## RESULTS ON CARBONS

The morphology and structure of carbon grains appear rather complex (Rotundi *et al.*, 1998). Amorphous carbon smoke is formed by spherical (sphericity  $\sim 0.9 \div 1.0$ ) grains (diameter =  $7 \div 15$  nm) in *chain-like aggregates* (CLA). Although this is the most abundant form observed in our samples, other more ordered structures are present. *Poorly graphitised carbon* is formed by isolated carbon domains of loops and rings, delineated by a single graphite layer on smooth amorphous carbon. This is probably the result of auto-annealing during coagulation. *Bucky-onions* (diameter =  $10 \div 40$  nm) and *bucky-tubes* (100 x 10 nm in size) are, instead, products of the condensation process. Finally, rare *graphitic carbon ribbons* and *single-crystal carbon platelets* are the result of a localised pre-graphitisation process. The detailed analysis of the samples demonstrates that the CLA is the driving component in spectroscopic measurements (Rotundi *et al.*, 1998).

The mass extinction coefficient of carbon samples is characterised by a linear trend in the visible and some optical features in the UV range. A bump at 80 - 90 nm is due to a  $\sigma$ - $\sigma^*$  electronic transition, while

a feature at 200 - 260 nm is a  $\pi$ - $\pi^*$  electronic transition, whose exact position depends on the degree of grain internal order (Mennella *et al.*, 1995a,b). The medium IR (3 - 20  $\mu\text{m}$ ) presents bands typical of stretching and bending of C-H and C-C bonds. At longer wavelengths, down to the mm range, the spectral trend can be fitted by a  $\lambda^{-\alpha}$  power law, with spectral index  $\alpha = 1.1 \div 0.5$ , depending on bulk properties and on grain size and shape (Colangeli *et al.* 1995).

The previous results indicate that the production conditions significantly affect the structure of carbon-based materials. This, in turn, drives the behaviour of optical properties. In this respect, the presence of hetero-atoms, hydrogen in the first place, is a significant aspect, as it can be concluded by looking at the optical behaviour in the UV of carbon produced by varying the hydrogen content in the production chamber (Mennella *et al.*, 1997a) - see Figure 1.

According to the results summarised above, we can interpret the observed spectral modifications as a consequence of the different structural properties of grains produced under different ambient conditions. In particular, all the grains produced by arc discharge have a dominant aliphatic character, as demonstrated by the prevalence of the  $\text{sp}^3$  C-H stretch at 3.4  $\mu\text{m}$  over the  $\text{sp}^2$  C-H stretch at 3.3  $\mu\text{m}$ . Only for the BE sample the proportion seems inverted. On the other hand, the hydrogenated grains present a weak  $\pi$ - $\pi^*$  electronic transition around 200 nm, which evolves towards a more evident bump, shifted towards longer wavelengths as long as the hydrogen in the production chamber is reduced (see Figure 1). Actually, hydrogen inhibits the formation of large assemblies of C atoms, with consequent localisation of electronic carbon bonds and dominance of short range order.

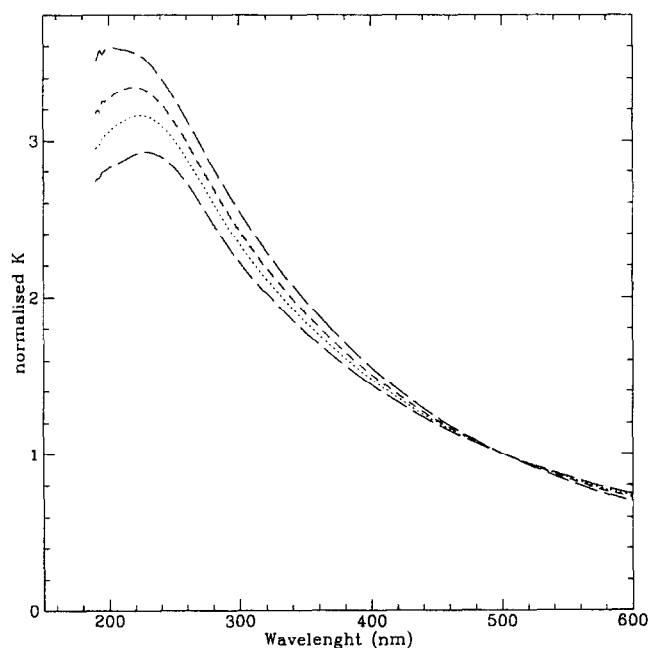


Fig. 1. Extinction of carbon grains produced in Ar- $\text{H}_2$  mixed atmosphere. From bottom to top: 0.4, 0.6, 0.8 and 1.0 % of  $\text{H}_2$  in Ar.

The relevance of production conditions on the final carbon grain properties is further confirmed by the comparison of our results with data obtained for other carbon based grains. As an example, carbon grains produced by laser pyrolysis of hydrocarbons (Herlin *et al.*, 1998) present a sharp and very intense 3.3  $\mu\text{m}$

feature. This suggests that such grains have a marked aromatic character and, at the same time, a lot of hydrogen bonded to the carbon structure.

Production in different conditions and/or by various methods allows us to obtain several types of grains, whose properties can be related to the operative boundary conditions. A further step ahead in the characterisation of materials is achieved by applying to synthesised grains the processes mentioned in the previous section.

The evolution of UV and IR optical properties of ACH2 grains after thermal annealing up to 800 °C demonstrates that this processing produces: a) a progressive hydrogen release; b) an internal grain structure modification. The neat effect is an “aromatisation” process in which  $sp^2$  clusters, forming the intimate structure of carbon grains, increase in number and grow in size. A similar aromatisation effect is induced on ACH2 by UV irradiation (Mennella *et al.*, 1996) and ion bombardment (Mennella *et al.*, 1997b), as shown by the UV bump variations. Interesting enough, the ion bombardment of ACAR, i.e. of grains with a partially “ordered” structure, induces an opposite effect, i.e. a tendency to move again towards a disordered arrangement of the carbon clusters forming the grains (Mennella *et al.*, 1997b).

Summing up for laboratory carbon grains, the hydrogenation inhibits the formation of ordered (large  $sp^2$ ) structures. The aromatisation process, i.e. the growth, in number and size, of  $sp^2$  clusters is promoted by condensation in hydrogen-poor ambient, thermal annealing, UV irradiation and ion bombardment. Ion bombardment has a double effect: highly disordered structures tend to become aromatic, while more ordered structures tend to become more disordered (de-clustering).

## RESULTS ON SILICATES

The silicates selected for our analyses allow us to compare materials pertaining to different classes. Actually, forsterite and fayalite are, respectively, the Mg-rich and the Fe-rich end-members of the olivine class,  $(Mg_x, Fe_{1-x})_2SiO_4$ , of silicates. Pyroxenes, instead, are characterised by a different chemical proportion,  $(Mg_x, Fe_{1-x})SiO_3$ , i.e. by a different internal structure. Enstatite is the Mg-rich end-member of this class.

SEM images show significant morphological differences for ground crystalline silicates and their counterparts synthesised by laser bombardment of the bulk materials. Ground crystalline silicates appear irregular in shape, have a power law size distributions,  $n(d) \propto d^{-p}$  with  $p \sim 2.1$ , and average diameters  $0.2 \div 0.6 \mu m$ . Silicates synthesised by laser bombardment occur in two different morphologies. Isolated spheroids have a size distribution power index  $p \sim 2.6$  and average diameter  $0.04 \div 0.07 \mu m$ . Aggregates of spheroid grains present a Gaussian distribution and an average diameter of  $0.01 \div 0.03 \mu m$ .

It is interesting to note that the EDX analysis demonstrates that the synthesised grains have the same elemental relative abundance as the parent materials, within experimental errors (see Table 2). This offers the opportunity to compare silicate grains with the same chemical formula but different structural order.

It is well known that the spectral characteristics of silicates, most interesting for comparisons with observations, are the Si-O stretching and Si-O-Si bending bands falling around 10 and 20  $\mu m$ , respectively. Examples of the mass absorption coefficient behaviour for the analysed materials are shown in Figures 2 to 4. The spectra show - as expected for crystalline materials - sharp features for all the ground samples. On the contrary, the synthetic grains mainly show broad bands centred around 10 and 20  $\mu m$ , as typical of amorphous silicates.

It must be noticed that the features at 10  $\mu\text{m}$  of the two crystalline olivines differ only in the detailed peak position, while a clearer profile difference is observed for the 20  $\mu\text{m}$  bands. On the contrary, olivines and enstatite have well distinct 10  $\mu\text{m}$  bands. These considerations imply that, in astronomical observations, the 10  $\mu\text{m}$  band can be more easily used to discriminate among different classes of silicates, while the 20  $\mu\text{m}$  band appears more appropriate to distinguish among materials of the same class (i.e. olivines). The same concept is true for amorphous silicates, even if the band broadening renders the differences less evident.

Interesting enough, thermal annealing in vacuum of amorphous Mg silicate smokes at around 1027 K produces a conversion towards a more crystalline phase, as evidenced by the IR band shape modifications (Hallenbeck *et al.*, 1998).

Table 2. Elemental abundance of elements derived from EDX analysis.

Material		Derived chemical formula
Forsterite	crystalline	$(\text{Mg}_{0.91}\text{Fe}_{0.08})_2\text{Si}_{1.01}\text{O}_4$
	synthetic	$(\text{Mg}_{0.91}\text{Fe}_{0.08})_2\text{Si}_{0.99}\text{O}_4$
Fayalite	crystalline	$(\text{Mg}_{0.07}\text{Fe}_{0.85})_2\text{Si}_{1.05}\text{O}_4$
	synthetic	$(\text{Mg}_{0.08}\text{Fe}_{0.91})_2\text{Si}_{0.99}\text{O}_4$
Enstatite	crystalline	$(\text{Mg}_{0.85}\text{Fe}_{0.08})\text{Si}_{0.91}\text{O}_3$
	synthetic	$(\text{Mg}_{0.75}\text{Fe}_{0.11})\text{Si}_{0.88}\text{O}_3$

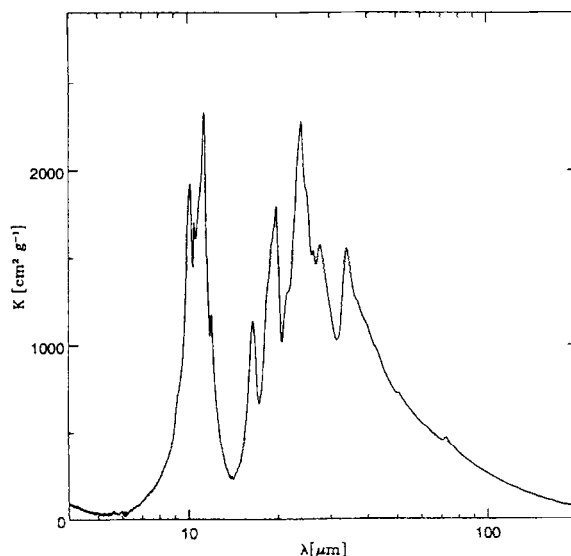


Fig. 2. Mass absorption coefficient of crystalline forsterite grains.

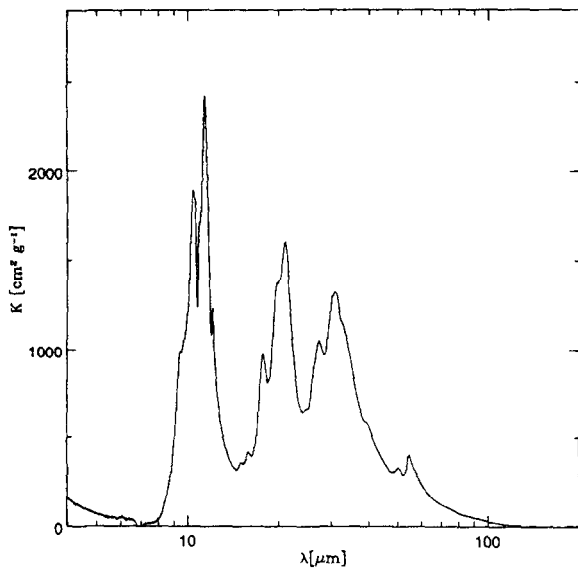


Fig. 3. Mass absorption coefficient of crystalline fayalite grains.

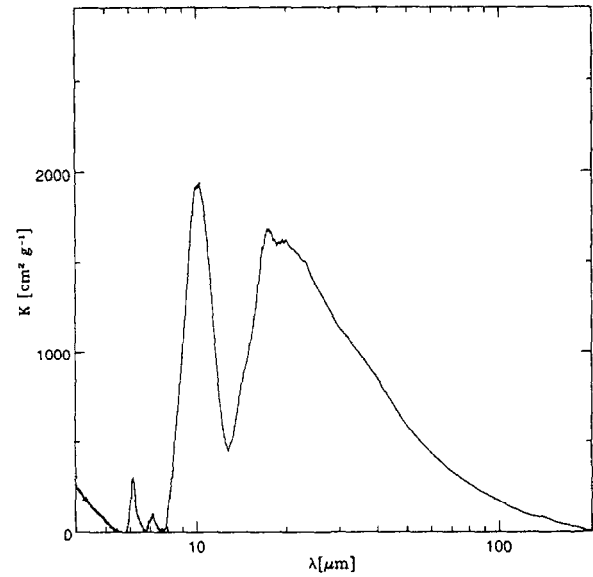


Fig. 4. Mass absorption coefficient of synthetic fayalite grains.

## ASTROPHYSICAL APPLICATIONS AND FINAL CONSIDERATIONS

The results reported in the previous sections offer a wide set of data concerning carbon-based and silicate grains, potentially valid for astrophysical applications. It must be recalled that it is not our intention to state that the analogues produced in laboratory are actually present in space. However, the behaviour of spectral features, observed for laboratory samples in dependence of morphological and structural properties, must be considered generally valid. Therefore, similar characteristics must be expected in space as a function of environment and active processes.

As an example of the application of laboratory spectra to observed features, we consider the recent ISO observations of comet Hale-Bopp (Crovisier *et al.*, 1997). They show sharp emission features, in the medium and far infrared, attributed to crystalline silicate grains. As mentioned in the Introduction, cometary grains can be expected to be fluffy (as our laboratory particles) silicate-carbon aggregates. This would imply a careful modelling of optical properties for such a complex structure (Hage & Greenberg, 1990, Bazell & Dwek, 1990, Stognienko *et al.*, 1995). However, under the hypothesis of highly porous (porosity  $P \approx 0.95$ ) aggregates formed by sub-micron grains, the observed flux can be simulated by a simple sum of independent terms for different components (Ossenkopf, 1991, Kozasa *et al.*, 1992):

$$F(\lambda) = (\beta_{AC}K_{AC} + \beta_{ForC}K_{ForC} + \beta_{ForA}K_{ForA} + \beta_{EnsA}K_{EnsA}) B(\lambda, T_1) + \delta_{LG} Q_{LG} B(\lambda, T_2) \quad (1)$$

Here,  $K$  is the mass absorption coefficient,  $Q$  is the extinction efficiency,  $B(\lambda, T)$  is the Planck function,  $\delta$  is a dimensionless factor and  $\beta = M/\Delta^2$  is the mass column density, with  $M$  = mass of each dust component within the telescope beam and  $\Delta$  = Earth-comet distance at the time of observation. The labels characterise the different grain types used in the simulation: AC = amorphous carbon, ForC = crystalline forsterite, ForA = amorphous forsterite, EnsA = amorphous enstatite. The label LG characterises the large grain population. Actually, in Eq. (1) we have considered the contribution of two different grain populations. The first term of the sum refers to *submicron grains* responsible of the emission features, assumed very fluffy, with a high vacuum volume fraction (i.e.  $P \approx 1$ ), with no mantle and chemically well distinct in a scale of 0.1 - 0.2  $\mu\text{m}$ . The second term considers *large grains* (say, larger than 50  $\mu\text{m}$ ), responsible of the continuum emission and behaving as black bodies ( $Q_{LG} = 1$ ). By applying a non-linear least square fit to observational data by Eq. (1), we have determined the  $\beta$  and  $T$  quantities, which are considered free parameters in the fit. The results are reported in Table 3. For comparison, the equilibrium temperature,  $T_{BB}$ , of an isolated grain at the heliocentric distance of Hale-Bopp at the time of observation, is reported in the table. The mean square root of the fit is 0.02. The best fit is shown in Figure 5. We recall that Brucato *et al.* (1998) have already reported a fit of the Hale-Bopp observations by a mixture of amorphous carbon, crystalline and amorphous olivine. In the present simulation we have added the amorphous enstatite component, which appears necessary to improve the fit to the short wavelength wing of the 10  $\mu\text{m}$  band.

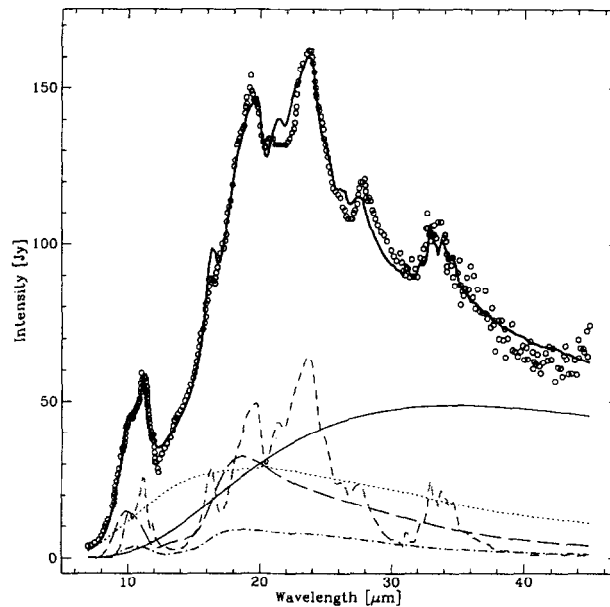


Fig. 5. Fit to comet Hale-Bopp emission spectrum (Crovisier *et al.*, 1997) - points - by laboratory data - continuous thick line. The contribution of the different components considered in the fit is also reported: large grains (continuous thin line), amorphous carbon (dotted line), amorphous enstatite (long dashed line), amorphous olivine (dash-dotted line) and crystalline olivine (dashed line).



Table 3. Results of the fit to the Hale-Bopp ISO spectrum (Crovisier *et al.*, 1997).

Grains	$\beta$ ( $\text{g cm}^{-2}$ )	$\delta$	Mass fraction				T (K)	$T_{\text{BB}}$ (K)
			AC	FORC	FORA	ENSA		
sub-micron	1.8E-16	---	0.18	0.41	0.08	0.33	201	163
> 50 $\mu\text{m}$	---	2.6E-13	---	---	---	---	146	163

If we apply the results obtained for the two populations of grains to determine the power index,  $\gamma$ , of the differential dust size distribution,  $g(s) \propto s^{-\gamma}$ , we obtain  $\gamma = 2.5$ , in agreement with the results obtained by Fulle (1998),  $2.5 < \gamma < 3.9$ , by analysing in-situ and ground-based data on several comets.

Clearly, the application shown above indicates the potential use of laboratory data to interpret astronomical observations. Generally speaking, it must be stressed that the results obtained in laboratory simulations can indicate the guidelines to follow to interpret cosmic dust composition and evolution. Several further steps must be undertaken in this respect. Among others, we recall the importance of accounting for the aggregation and/or isolation of grains in space.

#### ACKNOWLEDGEMENTS

This work has been supported under ASI, MURST and CNR contracts. We thank S. Inarta, N. Staiano and E. Zona for technical assistance during experiment execution.

#### REFERENCES

- Bazell, D., and E. Dwek, The effect of compositional inhomogeneities and fractal dimension on the optical properties of astrophysical dust, *Astrophys. J.*, **360**, 142 (1990).
- Brucato, J.R., L. Colangeli, V. Mennella, P. Palumbo, and E. Bussoletti, Silicates in Hale-Bopp: hints from laboratory studies, *Planet Spa. Sci.*, submitted (1998).
- Cardelli, J.A., D.M. Meyer, M. Jura, and B.D. Savage, The abundance of interstellar carbon, *Astrophys. J.*, **467**, 334 (1996).
- Colangeli, L., V. Mennella, P. Palumbo, A. Rotundi, and E. Bussoletti, Mass extinction coefficients of various submicron amorphous carbon grains: tabulated values from 40 nm to 2 mm, *Astron. Astrophys. Suppl. Ser.*, **113**, 561 (1995).
- Combes, M., J. Crovisier, T. Encrenaz, V.I. Moroz, and J. P. Bibring, The 2.5-12 micron spectrum of comet Halley from the IKS-VEGA experiment, *Icarus*, **76**, 404 (1988).
- Crovisier, J., K. Leech, D. Bockelée-Morvan, T.Y. Brooke, M.S. Hanner, B. Altieri, H.U. Keller, and E. Lellouch, The spectrum of comet Hale-Bopp (C/1995 O1) observed with the infrared space observatory at 2.9 AU from the Sun, *Science*, **275**, 1904 (1997).
- Disanti, M.A., M.J. Mumma, T.R. Geballe, and J. K. Davies, Systematic observations of methanol and other organics in comet P/Swift-Tuttle: Discovery of new spectral structure at 3.42 micron, *Icarus*, **116**, 1 (1995).
- Dwek, E., Can composite fluffy dust particles solve the interstellar carbon crisis?, *Astrophys. J.*, **484**, 779 (1997).
- Fulle, M., 46P/Wirtanen dust parameters constrained by in-situ and ground-based observations. *Planet. Space Sci.*, submitted (1998).

- Li, A., and J.M. Greenberg, A unified model of interstellar dust, *Astron. Astrophys.*, **323**, 566 (1997).
- Greenberg, J.M., Making a comet nucleus, *Astron. Astrophys.*, **330**, 375 (1998).
- Jenniskens, P., Optical constants of organic refractory residue, *Astron. Astrophys.*, **274**, 653 (1993).
- Hage, J.I., and J.M. Greenberg, A model for the optical properties of porous grains, *Astrophys. J.*, **361**, 251 (1990).
- Hallenbeck, S.L., J.A. Nuth III, and P.L. Daukantas, Mid-infrared spectral evolution of amorphous magnesium silicate smokes annealed in vacuum: comparison to cometary spectra, *Icarus*, **131**, 198 (1998).
- Hanner, M.S., K.L. David, and R.W. Russell, The 8-13 micron spectra of comets and the composition of silicate grains, *Astrophys. J.*, **425**, 274 (1994).
- Herlin, N., I. Bohn, C. Reynaud, M. Cauchetier, A. Golvez, and J.N. Rouzaud, Nanoparticles produced by laser pyrolysis of hydrocarbons: analogy with carbon cosmic dust, *Astron. Astrophys.*, **330**, 1127 (1998).
- Jessberger, E.K., and J. Kissel, Chemical properties of cometary dust and a note on carbon isotopes, in *Comets in the Post-Halley Era*, edited by R.L. Newburn, M. Neugebauer and J. Rahe, J., pp.1075-1092, Kluwer, Dordrecht (1991).
- Kozasa, T., J. Blum, and T. Mukai, Optical properties of dust aggregates, *Astron. Astrophys.*, **263**, 423 (1992).
- Malfait, K., C. Waelkens, L.B.F.M. Waters, B. Vandenbussche, E. Huygen, and M.S. De Graauw, The spectrum of young star HD 100546 observed with the Infrared Space Observatory, *Astron. Astrophys.*, **332**, L25 (1998).
- Mathis, J., Dust models with tight abundance constraints, *Astrophys. J.*, **472**, 643 (1996).
- Mennella, V., L. Colangeli, A. Blanco, E. Bussoletti, S. Fonti, P. Palumbo, and H.C. Mertins, A dehydrogenation study of cosmic carbon analogue grains, *Astrophys. J.*, **444**, 288 (1995a).
- Mennella, V., L. Colangeli, E. Bussoletti, G. Monaco, P. Palumbo, and A. Rotundi, On the electronic structure of small carbon grains of astrophysical interest; *Astrophys. J. Suppl. Ser.*, **100**, 149 (1995b).
- Mennella, V., L. Colangeli, P. Palumbo, A. Rotundi, W. Schutte, and E. Bussoletti, Activation of a UV resonance in hydrogenated amorphous carbon grains by exposure to UV radiation, *Astrophys. J.*, **464**, L191 (1996).
- Mennella, V., J.R. Brucato, E. Bussoletti, C. Cecchi Pestellini, L. Colangeli, E. Palomba, P. Palumbo, M. Robinson and A. Rotundi, Laboratory studies of cosmic dust analogues grains, in *Cosmic Physics in the Year 2000*, edited by S. Aiello, N. Iucci, G. Sironi, A. Treves and U. Villante, pp. 225-232, Ed. Compositori, Bologna (1997a).
- Mennella, V., G.A. Baratta, L. Colangeli, P. Palumbo, A. Rotundi, E. Bussoletti and G. Strazzulla, Ultraviolet spectral changes in amorphous carbon grains induced by ion irradiation, *Astrophys. J.*, **481**, 545 (1997b).
- Meyer, D.M., M. Jura, and J.A. Cardelli, The definitive abundance of interstellar oxygen, *Astrophys. J.*, **493**, 222 (1998).
- Mumma, M.J., M.A. Disanti, N. Dello Russo, M. Fomenkova, K. Magee-Sauer, C.D. Kaminski, and D.X. Xie, Detection of abundant ethane and methane, along with carbon monoxide and water, in comet C/1996 B2 Hyakutake: Evidence for interstellar origin, *Science*, **272**, 1310 (1996).
- Ossenkopf, V., Effective-medium theories for cosmic dust grains, *Astron. Astrophys.*, **251**, 210 (1991).
- Rotundi, A., F.J.M. Rietmaijer, L. Colangeli, V. Mennella, P. Palumbo, and E. Bussoletti, Identification of carbon forms in soot materials of astrophysical interest, *Astron. Astrophys.*, **329**, 1087 (1998).
- Snow, T.P., and A.N. Witt, Interstellar depletions update: where all the atoms went, *Astrophys. J.*, **468**, L65 (1996).
- Stognienko, R., Th. Henning and V. Ossenkopf, Optical properties of coagulated particles, *Astron. Astrophys.*, **296**, 797 (1995).
- Waelkens, C., et al., SWS observations of young main-sequence stars with dusty circumstellar disks, *Astron. Astrophys.*, **315**, L245 (1996).
- Waters, L.B.F.M., et al., Mineralogy of oxygen-rich dust shells, *Astron. Astrophys.*, **315**, L361 (1996).